Silicon (2022) 14:5847–5854
https://doi.org/10.1007/s12633-021-01247-5

ORIGINAL PAPER

A Small Size On-chip Temperature Sensor Based on a Microring Resonator

Cong Hu [1,3] · Yunying Shi [1,3] · Tian Zhou [2] · Chuanpei Xu [1,3] · Aijun Zhu [1,3]

Received: 14 April 2021 / Accepted: 28 June 2021 / Published online: 9 September 2021

Abstract

In this paper, a small size on-chip temperature sensor based on microring resonator (MRR) is introduced. The sensor consists of a small microring waveguide with a radius of 3.1 μm and a runway waveguide with the same bending radius. To a certain extent, it solves the problem that high sensitivity and small size cannot coexist in the current on-chip temperature sensor, and provides a reference scheme for the design of on-chip temperature sensor. The experimental results show that the sensitivity of the sensor is 100pm/ , which breaks through the limit of 83pm/ for single microring. The free spectral range (FSR) is 39.25nm, and the resolution ratio is 0.47 , the temperature measurement range is improved, and a better resolution ratio is obtained. The microring temperature sensor designed in this paper has high sensitivity and small size structure (only 360μm^2), which is suitable for temperature measurement of Very Large Scale Integration (VLSI). It has great research value and application potential in the field of System-on-Chip (SoC) temperature detection.

Keywords Microring resonator · On chip sensor · Temperature sensor · Thermooptic effect

1 Introduction

In recent years, with the rapid development of integrated circuit industry, the technology progress and the reduction of characteristic size make the interconnection line spacing smaller and smaller and the integration degree higher and higher, which makes the power density more difficult to manage, and the temperature has become an important problem of chip optimization [1]. At present, many optical sensors are used in on-chip temperature detection. Compared with traditional electrical sensors, optical sensors have the advantages of strong anti-electromagnetic interference ability, high resolution, small size and easy integration [2, 3], and have been widely used in sensor detection. In optical sensing, there are many choices of sensing structure, including photonic crystal [4, 5], Bragg grating [6], Slot waveguide [7], Mach-Zehnder interferometer [8], MRR [9], etc. The micro ring resonator has a compact structure, high sensitivity and selectivity, and the micro ring resonator sensor based on photonic crystal has also attracted the attention of researchers because of its high sensing performance. However, the optical interconnection between the photonic crystal sensor and other devices is very difficult when the sensor is integrated into the chip, The fabrication of photonic crystal devices is also inconvenient. The traditional waveguide microring resonator is easy to be realized by using the existing SOI technology, and it is more convenient to integrate with other devices. It is suitable for on-chip sensing and detection, and is favored by many researchers. Among them, the MRR has compact structure design, high sensitivity and selectivity, can be realized by using the existing Silicon-On-Insulator (SOI) technology, and is more suitable for on-chip system sensing detection, which has attracted much attention of researchers. Ding et al. [10] used a dual-polarization silicon MRR to simultaneously detect humidity and temperature on-chip. The RH and temperature response sensitivities of TE and TM polarization were 97.9pm/% RH, 325.1pm/% RH, 69.0pm/°C and 30.6pm/°C, respectively. However, the sensitivity was relatively low, which could not be fully applied to the detection of SoC. Wan et al. [11] studied an on-chip high sensitivity temperature

✉ Tian Zhou
1404490856@qq.com

[1] School of Electronic Engineering and Automation, Guilin University of Electronic Technology, Guilin, Guangxi 541004, China

[2] School of Electronic Information and Automation, Guilin University of Aerospace Technology, Guilin, Guangxi 541004, China

[3] Guangxi Key Laboratory of Automatic Detecting Technology and Instruments, Guilin, Guangxi 541004, China

sensor based on a dye-doped solid-state polymer microring laser. The sensor achieved a high sensing sensitivity of 228pm. At the same time, the sensor size was large, and the radius of the microring resonator reached 115.4 μm. Singha et al. [12] designed an electronic circuit microring based on chip temperature sensor is designed. It consists of several MRR connected in parallel fashion and investigated the wavelength shift of a MRR (due to thermo-optic and thermal expansion effects) with respect to an isolated MRR. They obtained a large sensing range (~40nm) and wavelength shift of 0.2nm/°C over a temperature range of 25 to 70 °C. Although this kind of microring sensor achieves high sensitivity, it uses multiple microrings cascaded at different positions of the circuit, which takes up a large chip system area in the design of the sensor.

It can be seen from the above examples and the microring resonator sensor reported at present that the microring resonator sensor will bring larger structure size while obtaining higher sensitivity, The sensitivity and structure size cannot be taken into account at the same time. Generally, the temperature sensing sensitivity of a single MRR is limited to 83pm/ [13, 14]. Many researchers improve the sensitivity of temperature sensors by cascading multiple microrings [15] or other special structures [16]. In this paper, a small-size on-chip temperature sensor is proposed based on the cascade mode of microring resonator waveguide and runway waveguide, which can achieve high sensitivity and reduce the size of the sensor.

2 Sensor Structure and Principle

Microring temperature sensor is based on the measurement of resonance wavelength shift or intensity change caused by temperature change at a fixed wavelength. Most microring resonator sensors use optical instruments to measure the resonance wavelength offset to obtain the change of monitoring quantity. The structure of the sensor designed in this paper is shown in Fig. 1(a), including a ring resonator and a racetrack resonator [2]. It is placed on the test circuit to sense the change of the environment temperature by measuring the shift of the output spectrum of light after resonance in the microring silicon waveguide, and calculate the temperature of the integrated circuit environment based on the amount of change. When the temperature in the circuit increases, the refractive index of the silicon-based microring waveguide changes because of the thermo optic effect of the waveguide material, which makes the spectrum of the output end of the microring sensor shift in different degrees at different temperatures. In addition to the thermo optic effect, the thermal expansion effect will also affect the shift of the output spectrum of the microring sensor, and the perimeter of the microring waveguide structure will change due to the thermal expansion.

Due to the tight confinement of SOI nanowaveguides to photons, two-photon absorption and free carrier absorption will be induced under picosecond high-intensity optical pulses, and heat will be generated in the absorption process, resulting in thermal optical effect [3]. The thermal nonlinearity of free carriers generated by two-photon absorption converts the optical power into phase shift, which can induce the change of refractive index in the microring resonator. The effect of these carriers is much faster than the thermal effect. Two-photon absorption is excited only in a small region where the light intensity reaches a specific threshold. In a microring resonator, the threshold intensity can be expressed as

$$I_{th} = {}^{\alpha}\!/_{\beta} \tag{1}$$

α and β are linear and quadratic absorption coefficients,0.01 m^{-1} and $8 \times 10^{-12} mW^{-1}$, respectively. When the average intensity in the resonator is $I_{res} < I_{th}$, because silicon has very low thermal contact resistance and very low linear attenuation coefficient, the effect of two-photon absorption on the sensor can be ignored. When the average intensity in the resonator is $I_{res} > I_{th}$, the temperature rise generated by two-

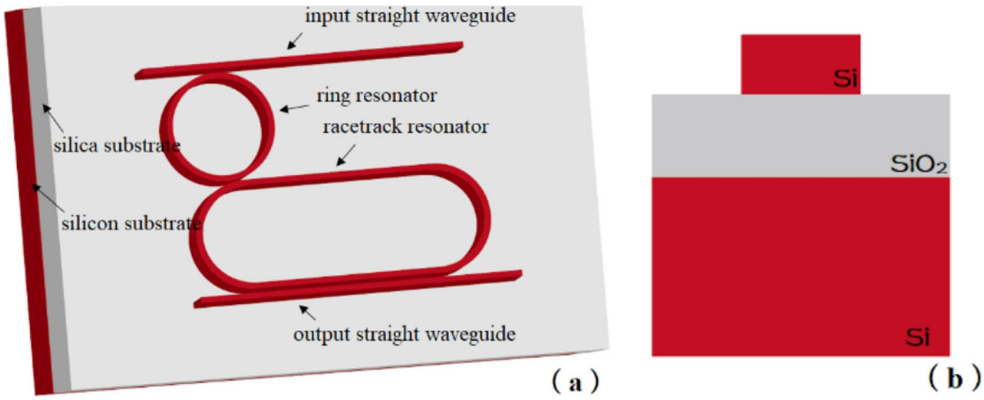

Fig. 1 Structure of temperature sensor based on MRR

photon absorption can be expressed by the Eq.

$$\Delta T = \frac{\tau_{th}\alpha_{TPA}}{\rho_{Si}C_{Si}} I_{res} \quad (2)$$

ΔT is the temperature change value, α_{TPA} is the two-photon absorption loss, $\rho_{Si} = 2.3 \times 10^{-3} kg/m^3$ is the mass density of silicon, C_{Si}=705J/(kg/K) is the specific heat capacity of silicon and $\tau_{th} = 1\mu s$ is the heat dissipation time. It can be seen from the formula that the two-photon absorption generation will generate a certain amount of heat, but it's much less heat than an integrated circuit, it has little influence on the temperature test of the integrated circuit [17, 18].

The cross section of the waveguide material of the silicon-based MRR temperature sensor is shown in Fig. 1(b). The effective refractive index of the silicon-based microring material under the thermo optic effect can be calculated by the following Eq:

$$n_{eff} = n(\lambda, T)[1 + C_1(T - T_0)] \quad (3)$$

Where $n(\lambda, T)$ is the refractive index of the waveguide at room temperature, $C_1 = \frac{1}{n(\lambda,T_0)} \frac{\partial n}{\partial T}$ is the thermo-optic coefficient of silicon-based waveguide, T is the monitoring temperature,T_0 is normal temperature. In this paper, the thermo-optic coefficient of silicon is 1.86×10^{-4} /°C [11, 12, 14].

The thermo optic effect will change the refractive index of the waveguide according to the change of temperature, which will shift the output spectrum of the sensor. The thermal expansion effect will change the length of the waveguide, which will also affect the output spectrum of the sensor. The relationship between waveguide length and temperature in different environments can be expressed as follows:

$$L = e^{\alpha T + C_0} \quad (4)$$

Where $\alpha = \frac{1}{L}\frac{dL}{dT} = 2.63 \times 10^{-6}/k$ is the coefficient of thermal expansion, $C_0 = InL_0 - 2.63 \times 10^{-6} T_0$, L_0 is the length of the waveguide at room temperature. Because the thermal expansion coefficient is two orders of magnitude smaller than the thermo-optic coefficient, and the waveguide structure is very small, the effect of the thermal expansion coefficient on the resonant spectral shift is very small and can be ignored.

In general, the output spectrum drift is mainly caused by the change of waveguide length and refractive index. The equation is as follows:

$$\frac{\Delta\lambda}{\lambda} = \frac{\Delta n}{n} + \frac{\Delta L}{L} \quad (5)$$

$$\Delta\lambda = \Delta\lambda_n + \Delta\lambda_L = \left[\frac{\frac{\partial n_{eff}}{\partial T} + n_{eff}\left(\frac{\partial L}{\partial T}\right)\left(\frac{1}{L}\right)}{n_g}\right] \quad (6)$$

Where $\Delta\lambda$ is the drift of the output spectrum of the sensor, ΔL is the change of the waveguide length of the microring resonator, $\triangle$ n is the change of the waveguide refractive index, $n_g = n_{eff} - \lambda_{res}\left(\frac{\partial n_{eff}}{\partial \lambda_{res}}\right)$ is the group refractive index of the microring waveguide.

According to the coupled mode theory and the transfer matrix method, the mathematical model of cascade temperature sensor with ring resonator and runway resonator is established. As shown in Fig. 2, the sensor can be divided into three parts: straight waveguide and ring waveguide coupling (coupling region (a)), ring waveguide and runway waveguide coupling (coupling region (b)) and straight waveguide and straight waveguide coupling (coupling region (c)). The incident light enters the waveguide from the input port and is coupled into the microring resonator. After resonating in the microring, the light wave exits the waveguide sensor from the output port, and the wavelength drift is monitored at the output port. Because the distance between the two waveguides is different, the coupling coefficient at different points of the waveguide is also different. When we analyze the amplitude coupling between ring waveguide and straight waveguide or ring waveguide and ring waveguide, we divide the coupling region of ring waveguide into many small segments. Because the coupling region of the ring waveguide is divided into small coupling analysis segments, we set the distance between the two ends of the coupling waveguide as a constant, so that the bending coupling can be equivalent to the directional coupling. Therefore, the coupled mode Eq of directional coupling can be obtained:

$$\frac{dR(z)}{dz} = j\delta R(z) - jK_{12}S(z) \quad (7)$$

$$\frac{dS(z)}{dz} = -j\delta S(z) - jK_{21}R(z) \quad (8)$$

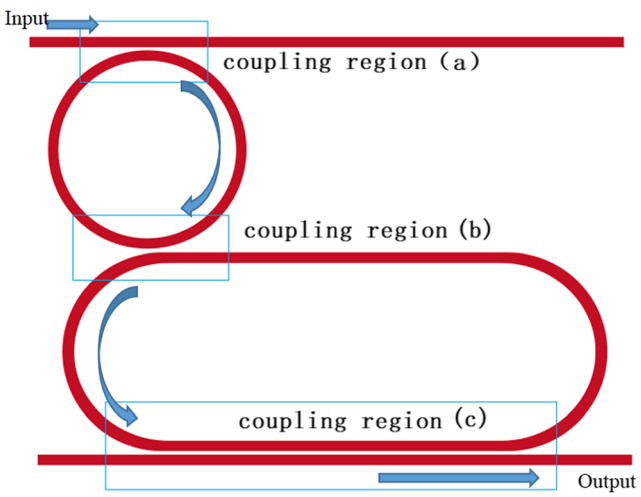

Fig. 2 Waveguide coupling region of microring temperature sensor

Table 1 Waveguide parameters

	Radius(μm)	Width(μm)	Height(μm)	Separation(μm)	Length(μm)
Ring waveguide	3.1	0.475	0.18	0.1	
Racetrack waveguide	3.1	0.475	0.18	0.1	9.734
Straight waveguide		0.475	0.18	0.1	20
SiO_2 substrate			4		
Si substrate			40		

Where δ is the phase mismatch factor, $2\delta = [(\beta_2 - \beta_1) + (M_2 - M_1)], M_1, \ M_2$ is the self coupling coefficient of two waveguides in the coupling region, $K_{12}, \ K_{21}$ is the coupling coefficient between two waveguides, and there is $K_{21} = K_{12}^*$. The waveguides of the sensor designed in this paper are all made of silicon material, that is, the parameters of the two waveguides in the coupling region are the same, and there is $\beta_1 = \beta_2 = \beta$, $M_1 = M_2 = M$, $K_{12} = K_{21} = K$, so $\delta = 0$. Then the coupled mode Eq of the i-th segment is:

$$\frac{dR(z)}{dz} = -jK_iS(z) \tag{9}$$

$$\frac{dS(z)}{dz} = -jK_iR(z) \tag{10}$$

The mode coupling matrix equations of the two waveguides can be obtained by deriving and calculating Eqs. (9) and (10):

$$\begin{pmatrix} R_i \\ S_i \end{pmatrix} = \begin{bmatrix} cos\left[\int_{-L}^{z} K(z)dz\right] & -jsin\left[\int_{-L}^{z} K(z)dz\right] \\ -jsin\left[\int_{-L}^{z} K(z)dz\right] & cos\left[\int_{-L}^{z} K(z)dz\right] \end{bmatrix} \times \begin{pmatrix} R_{i-1} \\ S_{i-1} \end{pmatrix} \tag{11}$$

From this Eq, the coupling equation of waveguide can be obtained as follows:

$$\begin{pmatrix} R(L) \\ S(-L) \end{pmatrix} = \begin{bmatrix} t & -jk \\ -jk & t \end{bmatrix} \begin{pmatrix} R(-L) \\ S(-L) \end{pmatrix} \tag{12}$$

Table 2 Waveguide material parameters

	Si	SiO_2
Refractive index	3.48	1.44
Thermo-optic coefficient	1.86×10^{-4}/°C	1.0×10^{-5}/°C
Thermal expansion coefficient	2.5×10^{-6}/°C	5.6×10^{-7}/°C

Where $t = cos\left[\int_{-L}^{L} K(z)dz\right], k = sin\left[\int_{-L}^{L} K(z)dz\right]$, so $k^2 + t^2 = 1$.

For the coupling region (a) of the sensor waveguide structure in Fig. 2, the included Angle θ = 0 between the optical signals transmitted in the waveguide, the coupling coefficient of the waveguide coupling is K(z). For the coupling region (b), the angle between the two optical signals in the waveguide is the sum of the tilt angles of the two optical signals, that is, $\theta = \theta_1 + \theta_2 \neq 0$, from which the waveguide coupling coefficient can be obtained $K(z) = K_{\parallel} \cdot \cos(\Theta_1) \cdot \cos(\Theta_2)$, where $K_{\parallel}$ is the parallel coupling coefficient of the waveguide.

The coupling region (c) is the coupling between the straight runway waveguide and the straight communication waveguide. Because the two waveguides are close to each other, when the light wave in the runway waveguide changes, the disturbance will occur in the straight communication waveguide, and the coupling between the two modes begins. The coupling equation is

$$\frac{dA}{dz} = -jK_{ab}Bexp[-j(\beta_b - \beta_a)z] - jM_aA \tag{13}$$

$$\frac{dB}{dz} = -jK_{ba}Aexp[-j(\beta_a - \beta_b)z] - jM_bB \tag{14}$$

Where $K_{ab}, \ K_{ba}$ is the coupling coefficient of two waveguides, $\beta_a, \ \beta_b$ is the propagation constant, $M_a, \ M_b$ is:

$$M_{a,b} = \frac{\omega\epsilon_0}{4} \int_{-\infty}^{\infty} \left[n^2(x) - n_{a,b}^2(x)\right] \left[E_y^{(a,b)}\right]^2 dx \tag{15}$$

3 Simulation and Analysis

According to the structure design in the previous chapter, this paper carries out the experimental simulation on Lumerical FDTD. In the experiment, the radius of the microring waveguide is 3.1 μm, the radius of the curved part of the runway waveguide is 3.1 μm, and the length of the straight runway is 9.734 μm, the refractive index of Si material is 3.475, and that of SiO_2 material is 1.44 [12]. The parameters of the

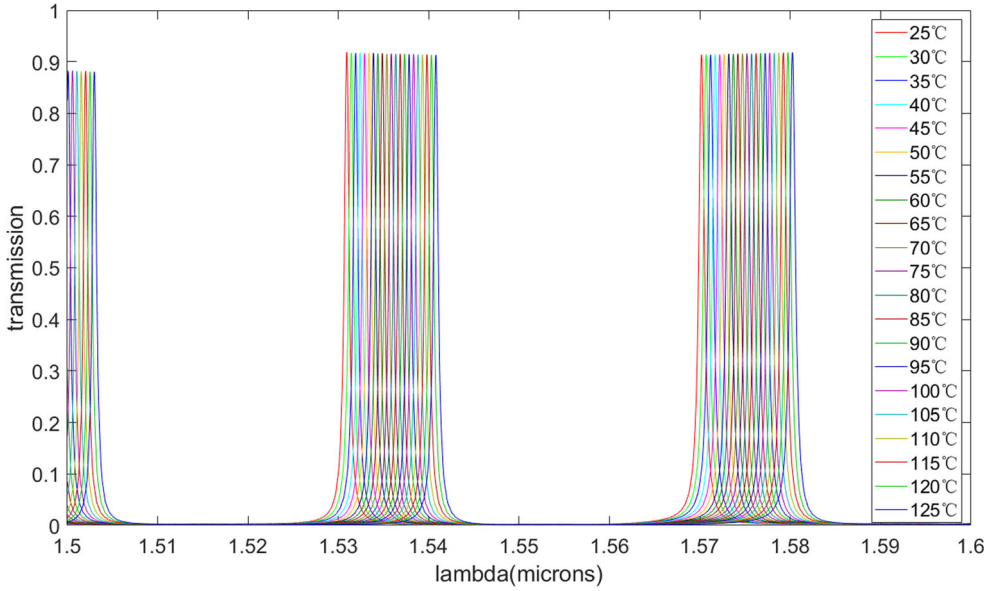

Fig. 3 The output spectrum of the microring sensor at different temperatures when the wavelength is 1.5 to 1.6 μm

simulation are shown in Tables 1 and 2. When the incident light wavelength is 1.5 to 1.6 μm, the output spectrum of the microring sensor under different temperature environment is obtained through experimental simulation, as shown in Fig. 3. In this band, two transmission regions can be seen clearly, and many transmission peaks can be seen in each transmission region. This is the transmission spectrum at 25 to 125 , in which the temperature difference between each two transmission peaks is 5 , and there are some transmission peaks at the wavelength of 1.5 μm. Figure 4 is an enlarged view of the resonance wavelength of the transmission peak in the 1.52 to 1.55 μm band. From these two figures, it can be seen that the transmission peak shifts with the increasing temperature. After measurement and calculation, the transmission peak of resonance wavelength shifts about 500pm every time the temperature rises 5 , that is to say, the temperature sensor designed in this paper has a sensitivity of 100pm/ in the SoC temperature sensing. As shown in Fig. 5, the broken line diagram of the resonant wavelength changing with temperature in the 1.52 to 1.55 μm waveband. From the broken line diagram of the resonant wavelength changing in the diagram, it can be seen that the wavelength changes almost linearly in the temperature range of 25 to 125 , that is, the temperature sensor has good linearity in this temperature range, and it can also be seen that the microring resonator has obvious characteristics in temperature sensing. Figure 6 shows the free spectrum range of the microring resonator sensor. After calculation, the free spectrum range of the microring resonator sensor

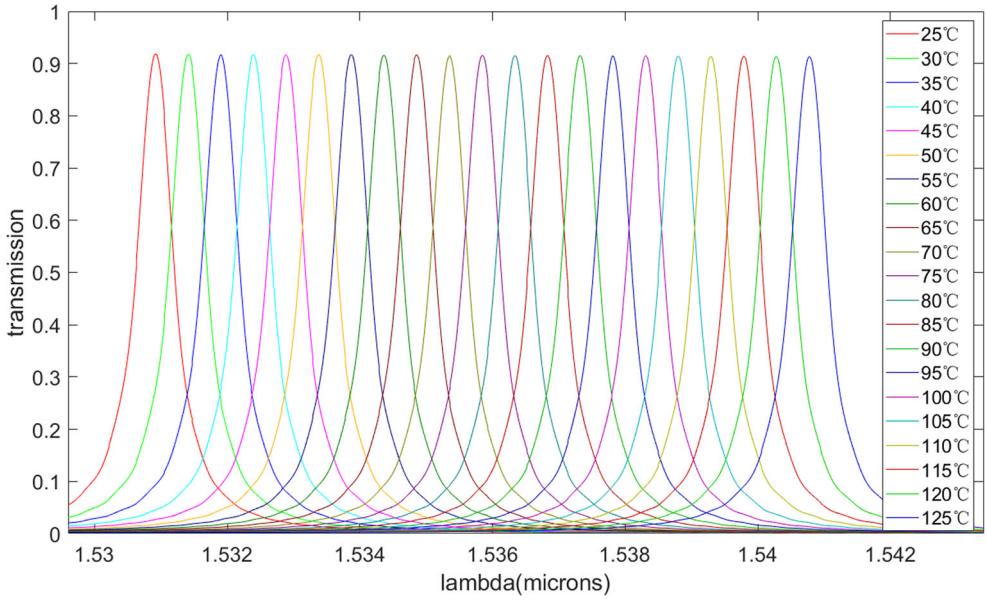

Fig. 4 Transmission spectra at different temperatures from 1.52 to 1.55 μm

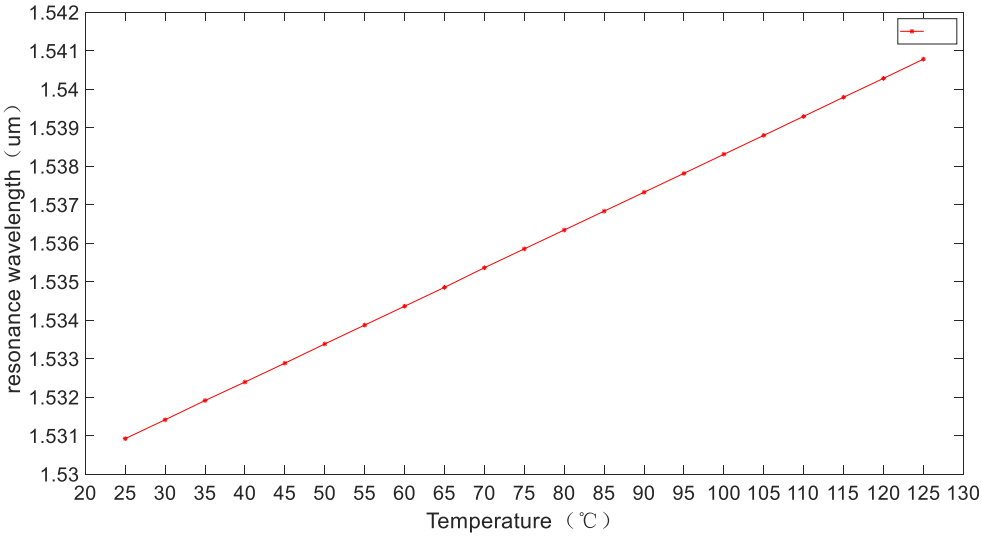

Fig. 5 The shift of transmission spectrum at different temperature

can reach 39.25nm, according to the previously measured 100pm/ sensing sensitivity, the measurement range of the sensor can reach 392.5 .The data comparison between the microring sensor designed in this paper and the recently reported MRR on-chip sensor is shown in Table 3. Compared with sensors designed by other researchers in the table, the sensitivity of our sensor is second only to Wan's [11] On-chip, high-sensitivity temperature sensors based on dye-doped solid-state polymer microring lasers. The sensitivity of the sensor designed by them is 228.6pm/ , in addition, the size of their MRR is relatively large, with a radius of 115.4 μm, which does not include the size of the peripheral channel waveguide. At present, integrated circuits are developing towards miniaturization, high integration and high density, such a large size is obviously not conducive to integration in SoC, which is not in line with the current trend of miniaturization of integrated circuit devices. In comparison, the sensor size designed by Ding [10], Zhang [19] and Weituschat [17] is more in line with the design trend of device miniaturization. Compared with their design, our sensor radius is smaller, and the whole sensor size is relatively small, which can better realize the integration of SoC. Although the sensor size in the table is only the radius of the microring, and there is no statistics on the size of the whole sensor, the size of each sensor can be roughly compared from the radius of the microring. In the aspect of sensor resolution, the sensors designed by Ding Z and Weituschat LM did not give specific resolution, while the sensors designed by Li W and Zhang C achieved better resolution, which were 0.35 and 0.25mk, respectively. The sensor designed in this paper also has a resolution of 0.47 , which can be normally monitored in the temperature monitoring of integrated circuit system environment.

4 Conclusions

In this paper, a compact and easily integrated microring resonator temperature sensor is introduced. The sensor is

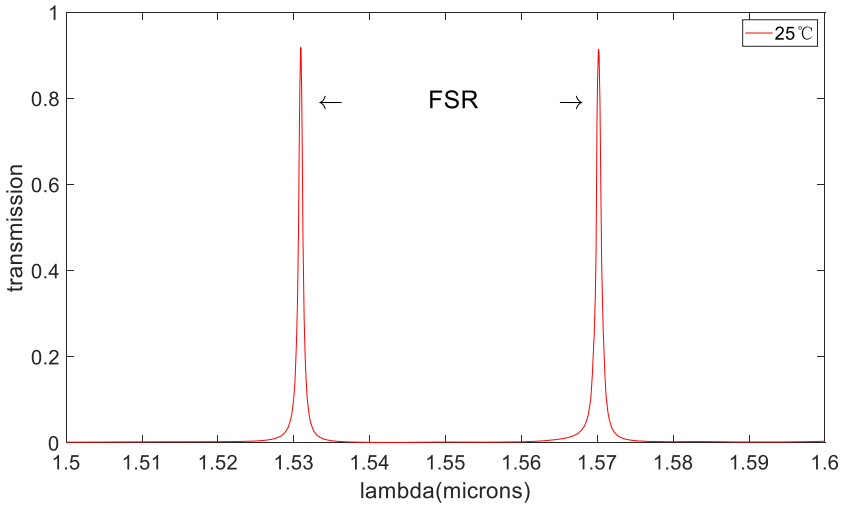

Fig. 6 Free spectral range (FSR)

Table 3 Comparison of results

	Wan [11]	Ding [10]	Zhang [19]	Weituschat [17]	This work
Sensitivity	228.6pm/°C	69.0pm/°C and 30.6pm/°C for TE and TM	75.3pm/°C	68.2pm/°C	100pm/°C
Resolution ratio	0.35°C		0.25mk		0.47°C
Microring radius	115.4 μm	20 μm	10 μm	10.485 μm	3.1 μm
Overall size	83980 μm^2	2816 μm^2	1176 μm^2	2050 μm^2	360 μm^2

composed of a microring waveguide and a runway waveguide, the radius of the microring is only 3.1 μm, and the area of the whole temperature sensor is only 360μm^2. It is very suitable for the application in integrated circuits. In this paper, the coupling principle and temperature sensing principle of the MRR sensor are analyzed theoretically, and the temperature in the circuit environment is obtained by measuring the shift of the transmission peak of the resonant wavelength. The simulation results show that the temperature response of the sensor is about 100pm/ , and it has good linearity, the FSR of 39.25nm is obtained, which widens the temperature measurement range and can be applied to a variety of temperature environments. Compared with other microring temperature sensors, the temperature sensor has higher temperature sensing sensitivity, compact structure, small volume, easy to integrate with other optical systems, suitable for large-scale integrated circuit temperature measurement. It has great research value and application potential in the field of SoC temperature detection.

Acknowledgements We are thankful to the reviewers for the valuable suggestion.

Authors' Contributions All the authors are equally contributed in the manuscript.

Funding This work is supported by National Natural Science Foundation of China (61861012), Guangxi Key Laboratory of Automatic Detecting Technology and Instruments (YQ21105), Science Foundation of Guilin University of Aerospace Technology (XJ20KT09) and Research Basic Ability Improvement Project for Young and Middle-aged Teachers of Guangxi Universities (2021KY0800).

Data Availability All of data and material are available.

Code Availability All of the required data from the utilized software can be delivered.

Declarations This article does not contain any studies involving animals or human participants performed by any of the authors.

Conflicts of Interest/Competing Interests There is no conflicts/competing of interests.

EthicsApproval We confirm the ethic approval.

Consent to Participate All of authors and contributors have consent for this article.

Consent for Publication All of authors and contributors have consent topublish in this journal.

References

1. Islam AKMM, Shiomi J, Ishihara T, Onodera H (2015) Wide-supply-range all-digital leakage variation sensor for on-chip process and temperature monitoring. IEEE J Solid State Circuits 50:2475–2490
2. Zhang L, Jie L, Zhang M, Wang Y, Xie Y, Shi Y, Dai D (2020) Ultrahigh-Q silicon racetrack resonators. Photon Res (Washington DC) 8:684
3. Bogaerts W, De Heyn P, Van Vaerenbergh T, De Vos K, Kumar Selvaraja S, Claes T, Dumon P, Bienstman P, Van Thourhout D, Baets R (2012) Silicon microring resonators. Laser Photon Rev 6:47–73
4. Zegadi R, Ziet L, Zegadi A (2020) Design of high sensitive temperature sensor based on two-dimensional photonic crystal. Silicon 12:2133–2139
5. Biswas U, Rakshit JK, Das J, Bharti GK, Suthar B, Amphawan A, Najjar M (2021) Design of an ultra-compact and highly-sensitive temperature sensor using photonic crystal based single micro-ring resonator and cascaded micro-ring resonator. Silicon 13:855–892
6. Zhao CY, Zhang L, Zhang CM (2018) Compact SOI optimized slot microring coupled phase-shifted Bragg grating resonator for sensing. Opt Commun 414:212–216
7. Kazanskiy NL, Khonina SN, Butt MA (2020) Subwavelength grating double slot waveguide racetrack ring resonator for refractive index sensing application. Sensors 20:3416
8. Tang T, Luo L (2016) Refractive index sensor of Mach–Zehnder interferometer based on thermo-optic effect of SOI waveguide. Optik 127:6366–6370
9. Javanshir S, Pourziad A, Nikmehr S (2019) Optical temperature sensor with micro ring resonator and graphene to reach high sensitivity. Optik 180:442–446
10. Ding Z, Liu P, Chen J, Dai D, Shi Y (2019) On-chip simultaneous sensing of humidity and temperature with a dual-polarization silicon microring resonator. Opt Express 27:28649
11. Wan L, Chandrahalim H, Chen C, Chen Q, Mei T, Oki Y, Nishimura N, Guo LJ, Fan X (2017) On-chip, high-sensitivity temperature sensors based on dye-doped solid-state polymer microring lasers. Appl Phys Lett 111:61109
12. Singha S, Bhowmik BB (2018) On-chip photonic temperature sensor using micro ring resonator. 2018 Fifteenth International

Conference on Wireless and Optical Communications Networks (WOCN)
13. Kim G, Lee H, Park C, Lee S, Lim BT, Bae HK, Lee W (2010) Silicon photonic temperature sensor employing a ring resonator manufactured using a standard CMOS process. Opt Express 18: 22215–22221
14. Xu H, Hafezi M, Fan J, Taylor JM, Strouse GF, Ahmed Z (2014) Ultra-sensitive chip-based photonic temperature sensor using ring resonator structures. Opt Express 22:3098–3104
15. Kim H, Yu M (2016) Cascaded ring resonator-based temperature sensor with simultaneously enhanced sensitivity and range. Opt Express 24:9501
16. Tian C, Zhang H, Li W, Huang X, Liu J, Huang A, Xiao Z (2020) Temperature sensor of high-sensitivity based on nested ring resonator by Vernier effect. Optik 204:164118
17. Weituschat LM, Dickmann W, Guimbao J, Ramos D, Kroker S, Postigo PA (2020) Photonic and thermal modelling of microrings in silicon, diamond and GaN for temperature sensing. Nanomaterials 10:934
18. Ma C, Mookherjea S (2020) Prospects for photon-pair generation using silicon microring resonators with two photon absorption and free carrier absorption. OSA Continuum 3(5):1138
19. Zhang C, Kang G, Xiong Y, Xu T, Gu L, Gan X, Pan Y, Qu J (2020) Photonic thermometer with a sub-millikelvin resolution and broad temperature range by waveguide-microring Fano resonance. Opt Express 28:12599–12608